Edited by
Stig Lundqvist
Norman H. March
and
Mario P. Tosi

ORDER AND CHAOS IN NONLINEAR PHYSICAL SYSTEMS

Order and Chaos in Nonlinear Physical Systems

Edited by

Stig Lundqvist
Chalmers University of Technology
Göteborg, Sweden

Norman H. March
University of Oxford
Oxford, England

and

Mario P. Tosi
International Center for Theoretical Physics
Trieste, Italy

Springer Science+Business Media, LLC

Library of Congress Cataloging in Publication Data

Order and chaos in nonlinear physical systems.
(Physics of solids and liquids)
Bibliography: p.
Includes index.
1. Order-disorder models. 2. Chaotic behavior in systems. 3. Nonlinear theories. I. Lundqvist, Stig, 1925- . II. March, Norman H. (Norman Henry), 1927- . III. Tosi, M. P. IV. Series.
QC173.4.073073 1988 003 88-15113
ISBN 978-1-4899-2060-7

ISBN 978-1-4899-2060-7 ISBN 978-1-4899-2058-4 (eBook)
DOI 10.1007/978-1-4899-2058-4

Originally Published by Plenum Press, New York in 1988
Softcover reprint of the hardcover 1st edition 1988

12

Renormalization Description of Transitions to Chaos

P. Cvitanović

12.1. Introduction

The aim of this chapter, and the following one, is to review the developments which have greatly increased our understanding of chaotic dynamics during the past decade, and given us new concepts and modes of thought that, we hope, will have far-reaching repercussions in many different fields.

Once it was believed that given the initial conditions, we knew what a deterministic system would do far into the future. That was immodest. Today it is widely appreciated that given infinitesimally different starting points, we often end up with wildly different outcomes. Even with the simplest conceivable equations, almost any nonlinear system will exhibit chaotic behavior.

Confronted today with a potentially turbulent nonlinear dynamical system, we analyze it through a sequence of three distinct steps. First, we determine the intrinsic *dimension* of the system—the minimum number of degrees of freedom necessary to capture its essential dynamics. If the system is very turbulent (its attractor is of high dimension) we are, at present, out of luck. We know only how to deal with the transitional regime between regular motions and weak turbulence. In this regime the attractor is of low dimension, the number of relevant parameters is small, and we can proceed to the second step; we classify all the motions of the system by a hierarchy whose successive layers require increased precision and patience on the part of the observer. We call this classification the *symbolic dynamics* of the system: the following chapter shows how to do this for the Hamiltonian systems, and in this chapter we take the period n-tuplings and circle maps as instructive examples.

P. Cvitanović • Institute of Theoretical Physics, Chalmers University of Technology, S-412 96 Göteborg, Sweden.

Though the dynamics might be complex beyond belief, it is still generated by a simple deterministic law and, with some luck and intelligence, our labeling of possible motions will reflect this simplicity. If the rule that gets us from one level of the classification hierarchy to the next does not depend on the level, the resulting hierarchy is self-similar, and we can proceed with the third step: investigate the *scaling structure* of the dynamical system. This is the subject of the present chapter.

The scaling structure of a dynamical system is encoded into the *scaling functions.* The purpose of scaling functions is twofold:

For an experimentalist, they are the theorist's prediction of the motions expected in a given parameter and phase-space range. Given the observed motions up to a given level, the symbolic dynamics predicts what motions should be seen next, and the scaling functions predict where they should be seen, and what precision is needed for their observation.

For a theorist, the scaling functions are the tool which resolves asymptotically the fine structure of a chaotic dynamical system and proves that the system is indeed chaotic, and not just a regular motion of period exhausting the endurance of an experimentalist. Furthermore (and that is theoretically very sweet), the scalings often tend to *universal* limits. In such cases, the finer the scale, the better the theorist's prediction! So what *a priori* appears to be an arbitrarily complex dynamics turns out to be something very simple, and common to many apparently unrelated phenomena.

This is the essence of the recent progress here: large classes of nonlinear systems exhibit transitions to chaos which are *universal* and *quantitatively* measurable in a variety of experiments. This advance can be compared to past advances in the theory of solid-state phase transitions (cf. Chapter 10); for the first time we can predict and measure "critical exponents" for turbulence. But the breakthrough consists not so much in discovering a new set of scaling numbers, as in developing a new way to do physics. Traditionally we use regular as zeroth-order approximations to physical systems, and account for weak nonlinearities perturbatively. We think of a dynamical system as a smooth system whose evolution we can follow by integrating a set of differential equations. The new insight is that the zeroth-order approximations to strongly nonlinear systems should be quite different. They show an amazingly rich structure which is not at all apparent in their formulation in terms of differential equations. However, these systems do show self-similar structures which can be encoded by universality equations of a type which we will develop here.

As there is already much good literature on this subject, there is no point in reproducing it here. Instead, we provide the references which cover the same ground. However, it must be realized that the essence of this subject is incommunicable in print; here the intuition is developed by computing.

An introduction to the subject is provided by either of the two general reprint collections: one edited by Cvitanović,[1] and the other by Hao Bai-Lin.[2] Even though the selections overlap in only a few articles, both collections

contain introductory overviews, the fundamental theoretical papers, and the most important experimental observations.

The theory of period-doubling universal equations and scaling functions is most helpfully developed in Kenway's notes on Feigenbaum's lectures.[3] Another excellent text is the Collet and Eckmann monograph.[4]

The universality theory for complex period n-tuplings is developed by Cvitanović and Myrheim.[5]

A nice discussion of circle maps and their physical applications is given by Jensen *et al.*[6] and Bohr *et al.*[7] The universality theory for golden mean scalings was developed by Shenker,[8] Feigenbaum,[9] and Ostlund.[10] The scaling functions for circle maps are discussed by Cvitanović.[11] The above authors cover all of the theory discussed in this chapter. Experimental and theoretical advances can be swiftly appraised by scanning the *Physical Review Letters*, *Physics Today* "Search and Discovery" section, and the front pages of *The New York Times*!

12.2. Complex Universality

In this section (based on work in collaboration with Myrheim[5]), we develop the universality theory for period n-tuplings for complex maps.[12,13] This example is chosen for its beauty; here one should be able to visualize the renormalization transformations and the universal scalings as encodings of the self-similar patterns generated by the dynamics of the system.

We shall study metric properties of the asymptotic iterates of

$$z_{n+1} = f(z_n) \tag{12.2.1}$$

where $f(z)$ is a polynomial in the complex variable z with a quadratic critical point, i.e., with power-series expansion of the form

$$f(z) = a_0 + a_2(z - z_c)^2 + \cdots \tag{12.2.2}$$

Typical model mappings of this type are

$$f(z) = p + z^2 \tag{12.2.3}$$

$$f(z) = \lambda z(1 - z) \tag{12.2.4}$$

When such mappings are used to model dynamical systems with z a real variable and the "nonlinearity" parameter p real, the asymptotic attractor is conveniently represented by a "bifurcation tree," i.e., by a two-dimensional plot with p as one axis and values of the asymptotic iterates for given p plotted along the other axis.

It is not possible to describe asymptotics of complex iterations in this way, as their iteration space has two (real) dimensions, and period n-tuplings

are induced by tuning a pair of (real) parameters. To describe the asymptotic iterates of complex maps we proceed in two steps.

First, we describe the *parameter* space by its *Mandelbrot set M.* The Mandelbrot set[14,15] is the set of all values of the mapping parameter [parameter p in the model mapping (12.2.3)] for which iterates of the critical point do not escape to infinity. [A *critical point* z_c is a value of z for which the mapping $f(z)$ has vanishing derivative, $f'(z_c) = 0$. In equation (12.2.3) $z = 0$ is the critical point.] The Mandelbrot set for the mapping (12.2.4) is plotted in Figure 12.1.

Second, we characterize the *asymptotic iterates* for a given value of the parameter either by their *basin of attraction,* or by their *attractor.* The basin of attraction K is the set of all values of z which are attracted toward the attractor under iteration by $f(z)$. A typical basin of attraction is plotted in Figure 12.2. The boundary of K, or the *Julia set J,* is the closure of all unstable fixed points of all iterates of $f(z)$.

Theorem. For parameter values within the Mandelbrot set M, the Julia set J is connected. If all critical points iterate to infinity, J is a Cantor set.

If the nth iterate of $f(z)$ equals z, the set of points $z_k = f^k(z_0)$, $k = 0, 1, 2, \ldots, n-1$ form a periodic orbit (or cycle) of length n. If

$$|df^n(z_k)/dz_k| < 1 \tag{12.2.5}$$

the orbit is *attractive.* The *attractor L* is the periodic orbit $z_0, z_1, \ldots, z_{n-1}$. If

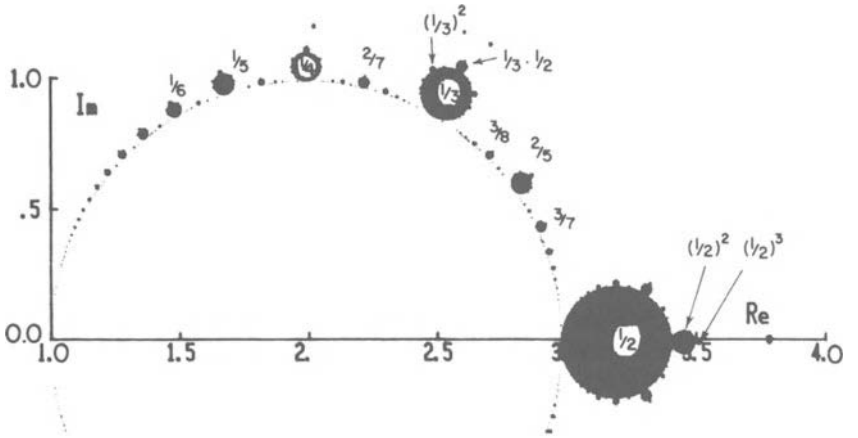

Figure 12.1. The Mandelbrot set M is the region in the complex parameter plane for which the critical point of the mapping (12.2.4) does not iterate away to infinity. Inside the big circle (left open for clarity) iterations converge to a fixed point. The full region has two symmetry axes, Re $\lambda = 1$ and Im $\lambda = 0$, so only one quarter is shown. The usual period-doubling sequence is on the real axis. The winding numbers of the periodic orbits corresponding to larger leafs of M are indicated. See Mandelbrot[15] for detailed scans of this set.

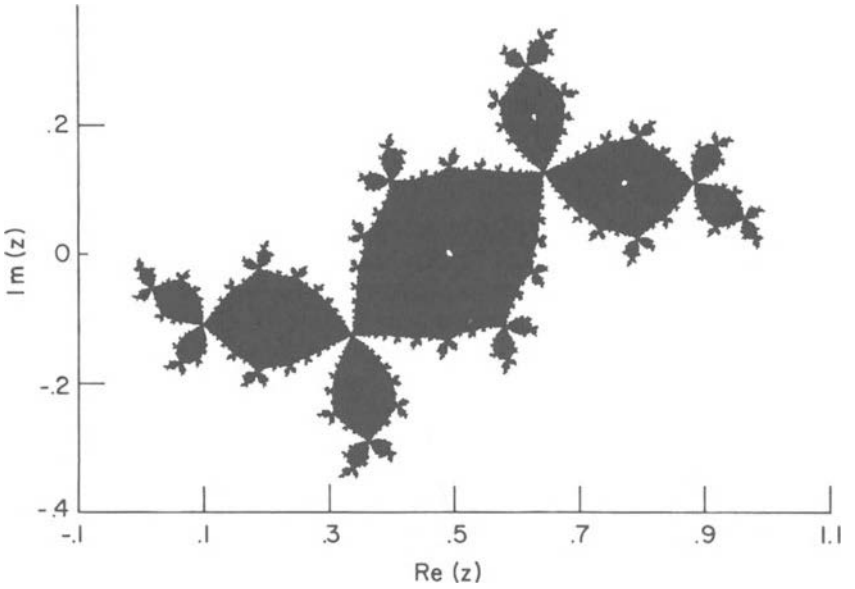

Figure 12.2. The basin of attraction for the superstable 3-cycle of mapping (12.2.4). Any initial z from the black region converges toward the superstable 3-cycle, denoted by the three white dots. The basin of attraction for mapping (12.2.3) superstable 3-cycle is the same, up to a coordinate shift and rescaling.

the derivative (12.2.5) is vanishing, the orbit is *superstable*, and (by the chain rule) a critical point is one of the cycle points. For polynomial mappings $z = \infty$ plays a special role; it is always a superstable fixed point. The following theorem eases attractor searches:

Theorem. The basin of attraction K contains at least one critical point.

The precise shape of the Mandelbrot set M depends on $f(z)$, but it always resembles a cactus; see Figure 12.1. Here we are not so much interested in the entire M, as in the *Mandelbrot cactus*, the set of connected components of M generated from a single fixed point by all possible sequences of all possible period n-tuplings.

To summarize, the parameter dependence of asymptotic iterates of mapping $f(z)$ is described by the Mandelbrot set M. For each point inside M, the asymptotic iterates are characterized by their basin of attraction K, the Julia set J, and the attractor L.

Now that the general setting is established, we can turn to a detailed study of the way in which a fixed point of the complex mapping (12.2.1) branches into an n-cycle. The fact that the same analysis applies to period n-tupling of any k-cycle into an nk-cycle will be seen to be the origin of the self-similarity of the Mandelbrot cactus.

The stability of a fixed point is given by

$$\rho = df(z)/dz \tag{12.2.6}$$

and we take, without loss of generality, the fixed point to be at $z = 0$, and $f(z)$ with a power-series expansion

$$f(z) = \rho z + a_J z^J \tag{12.2.7}$$

To bring the map into a standard form, we change the variable

$$w = z + b_J z^J \tag{12.2.8}$$

and "flatten" out the mapping close to the fixed point by choosing successively $b, b, \ldots$ in such a way that as many leading nonlinear terms as possible vanish in equation (12.2.7). If ρ is sufficiently close to the nth root of unity, $\omega = \exp(i2\pi m/n)$, and z is close to 0, the typical behavior of the new iteration function is the same as

$$f(z) = \rho z + z^{n+1} \tag{12.2.9}$$

This function has an n-cycle

$$z_J = \omega^J z_0, \qquad z_0^n = \omega - \rho \tag{12.2.10}$$

For $\rho = \omega$ this n-cycle coincides with the fixed point $z = 0$. In the neighborhood of $\rho = \omega$ we have

$$\begin{aligned} dz_n/dz_0 &= f'(z_0)f'(z_1)\cdots f'(z_{n-1}) \\ &= [\rho + (n+1)z_0^n]^n \\ &= 1 - (\rho - \omega)n^2/\omega + \cdots \end{aligned} \tag{12.2.11}$$

For $\rho = (1 + \varepsilon)\omega$ the n-cycle (12.2.10) of the mapping (12.2.9) is stable if

$$|1 - n^2\varepsilon| < 1 \tag{12.2.12}$$

while the fixed point is stable if

$$|1 + \varepsilon| < 1 \tag{12.2.13}$$

The mapping (12.2.9) is equivalent to equation (12.2.7) only for small z, so the above analysis of how a fixed point of equation (12.2.7) becomes unstable and branches into the n-cycle is valid only for infinitesimal $n\varepsilon$.

In conclusion, whenever a fixed point becomes unstable at $\rho = n$th root of unity, it branches into an n-cycle which immediately becomes stable. As any stable cycle becomes unstable in the same fashion, branching into a new stable cycle with a multiple of the original cycle length, and as any such cycle is stable inside a disk-like region in the complex parameter plane, the union of all these stability regions is a self-similar *Mandelbrot cactus.*

Next we turn to a study of infinite sequences of period n-tuplings, each branching characterized by the same ratio m/n.

As discussed above, a stable n^k-cycle becomes unstable and branches into an n^{k+1}-cycle when the parameter λ passes through a value such that the stability $\rho_k(\lambda)$ [as defined in equation (12.2.6.)] attains the critical value

$$\rho(\lambda) = \omega = \exp(i2\pi m/n) \tag{12.2.14}$$

For ρ sufficiently close to this value the system is modeled by equation (12.2.9). From equation (12.2.11) it follows that near the transition from an n^k-cycle to an n^{k+1}-cycle

$$\rho_{k+1} = 1 - (\rho_k - \omega)n^2/\omega + \cdots \tag{12.2.15}$$

hence

$$d\rho_{k+1}/d\lambda\big|_{\rho_{k+1}=1} = -(n^2/\omega)\, d\rho_k/d\lambda\big|_{\rho_k=\omega} \tag{12.2.16}$$

and at the transition there is a scale change by the complex factor $-n^2/\omega$ which is independent of k.

Each leaf of the Mandelbrot cactus Figure 12.1 corresponds to an m/n cycle, and the parameter value for the superstable m/n cycle corresponds to the center of the leaf. The above argument suggests that the leaf is n times smaller than the cactus, and that it is rotated by a phase factor $-1/\omega$. The very geometry of the Mandelbrot cactus, Figure 12.1, suggests such scaling. This scaling is not exact, because the above analysis applies only to the infinitesimal neighborhood of the junction of a leaf to the cactus; however, the evaluation of the exact scaling numbers shows that this is a rather good approximation to the exact scaling. We conjecture that $\delta_{m/n} \to n^2/\omega$ as $m/n \to 0$, exactly. This conjecture is supported by the numerical evaluation of the value of δ.[5]

The exact scaling is obtained by comparing values of the parameter λ corresponding to successive $(m/n)^k$ superstable cycles, i.e., λ values such that $\rho_k(\lambda_k) = 0$. As each cactus leaf is similar to the entire cactus, the ratios of the

sizes of the successive stability regions corresponding to successive $(m/n)^k$-cycles tend to a limit as $k \to \infty$:

$$\delta_{m/n} = \lim_{k\to\infty} (\lambda_k - \lambda_{k-1})/(\lambda_{k+1} - \lambda_k) \tag{12.2.17}$$

The scaling number δ tells us by how much we have to change the parameter λ in order to cause the next m/n period n-tupling. In particular, $\delta_{1/2} = 4.669...$ is the Feigenbaum δ for the period doublings in the real one-dimensional mappings.

Scaling in the parameter space (generalized Feigenbaum δ) is a consequence of the self-similarity of the Mandelbrot cactuses. In the same way the self-similarity of the Julia sets (or the asymptotic attractors) suggests a scaling law in the iteration space z, which we discuss next. This law will characterize the scales of successive trajectory splittings (generalized Feigenbaum α).

The self-similarity we are alluding to can be seen by comparing the basin of attraction for the superstable three-cycle, Figure 12.2, and for the superstable nine-cycle, Figure 12.3. In the latter figure the three-cycle basin of attraction is visible in the center, rotated and scaled down by a factor whose asymptotic limit is the generalization of Feigenbaum α to period triplings.

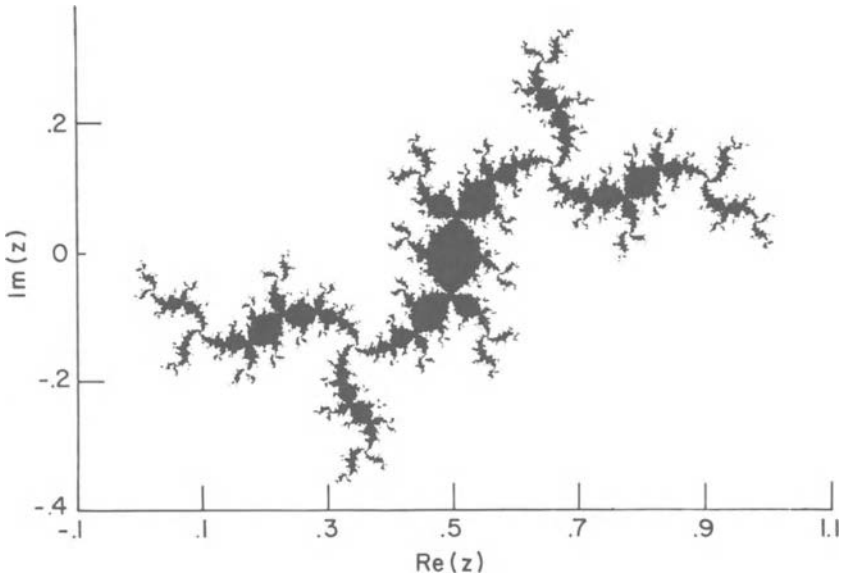

Figure 12.3. The basin of attraction for the superstable 9-cycle for iterates of the model mapping (12.2.4). The scaled down version of the 3-cycle basin of attraction, Figure 12.2, is visible in the center.

This scaling number α can be computed by comparing the successive superstable cycles at successive parameter values λ_k, λ_{k+1}. As $k \to \infty$, the sequence of values of λ converges to λ_∞, and the superstable n^k-cycles converge to an n^∞-cycle. The attractor is self-similar: the orbits on succeeding levels are related by rescaling and rotation by a complex number which asymptotically approaches

$$\alpha_{m/n} = \lim_{k\to\infty} (z_{n^k} - z_0)/(z_{n^{k+1}} - z_0) \tag{12.2.18}$$

α characterizes the scale of trajectory splitting at each period n-tupling. (For $m/n = \frac{1}{2}$ this is the Feigenbaum $\alpha = -2.5029\ldots$.)

So period n-tuplings are self-similar both in the iteration space and in the parameter space: not only does the asymptotic orbit resemble itself under rescaling and rotation by α, but also each leaf of the Mandelbrot cactus resembles the entire cactus under rescaling and rotation by δ.

These self-similarities can be described by means of the following three operations.

The first operation is a rescaling of the parameter and iteration spaces:

$$[Rf]_p(z) = af_{p/d}(z/a) \tag{12.2.19}$$

With the appropriate choice of complex numbers d (a), a leaf of the Mandelbrot cactus (a part of the attractor) can be rescaled and rotated to the size and the orientation of the entire cactus (entire attractor).

We fix the origin of p and z by requiring that $z = 0$ be a critical point of the mapping $f_p(z)$, and, for the parameter value $p = 0$, a superstable fixed point as well [equation (12.2.3) is an example of such mapping]. We fix the scale of p and z by requiring that the superstable m/n cycle occurs for the parameter value $p = 1$ and that

$$f_1(0) = 1 \tag{12.2.20}$$

The second operation shifts the origin of the parameter space to the center of the m/n-leaf of the Mandelbrot cactus (p corresponding to the superstable m/n cycle):

$$[Sf]_p(z) = f_{1+p}(z) \tag{12.2.21}$$

The third operation iterates $f_p(z)$ n times:

$$[Nf]_p(z) = f_p^n(z) \tag{12.2.22}$$

By definition, $[Sf]_0(z) = f_1(z)$ has a superstable m/n cycle, so its nth iterate has a superstable fixed point, $[\mathrm{NS}f]_0(0) = 0$.

The parameter shift S overlies the Mandelbrot cactus over its m/n leaf, and the Julia set for $[Nf]_1(z)$ resembles the Julia set for the superstable fixed point $f_0(z)$ (see Figures 12.2 and 12.3, for example). Finally we adjust the scale of the new M, J sets by requiring that the scale factors a, d in equation (12.2.19) are such that $[RNSf]_p(z)$ satisfies the same normalization condition (12.2.20) as the initial function $f_p(z)$. This shifting and rescaling is illustrated in Figure 12.4.

The combined effect of the rescaling, parameter shift, and iteration is summarized by the operator $T^* = RNS$;

$$[T^*f]_p(z) = af^n_{1+p/d}(z/a) \tag{12.2.23}$$

If we take a polynomial $f_p(z)$ and act on it with T^*, the result will be a longer polynomial with similar M and J sets. For a finite number of T^* operations the scaling numbers d and a depend on the choice of the initial mapping $f_p(z)$. If we apply T^* infinitely many times, a and d converge to the universal numbers α and δ, and $T^*f_p(z)$ converges to a one-parameter family

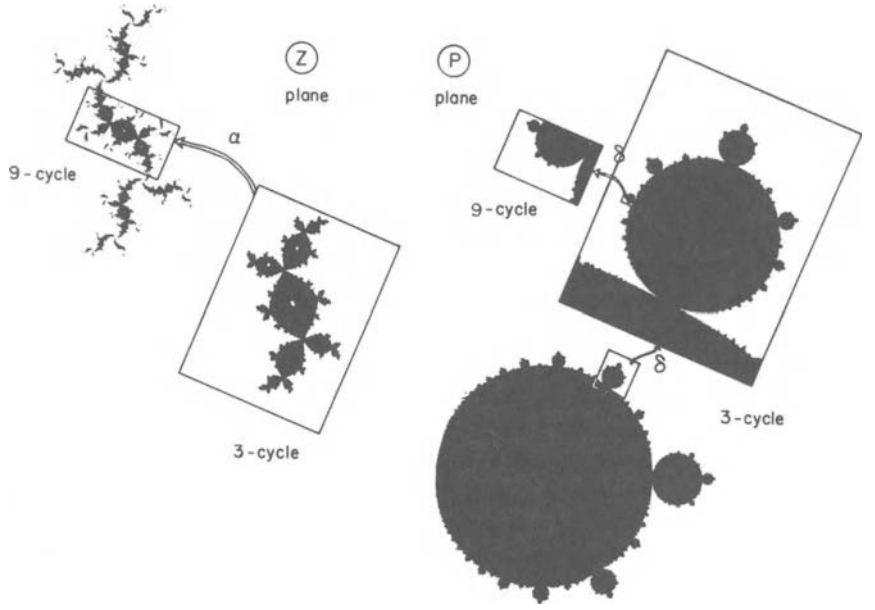

Figure 12.4. The unstable manifold method illustrated by period triplings. The parameter is shifted from the center of a cactus leaf to its $\frac{1}{3}$ leaf, the $\frac{1}{3}$ leaf is rescaled and rotated by δ, and the basin of attraction of third iterates is rescaled and rotated by α. The Mandelbrot cactus and the basin of attraction for the unstable manifold $g_p(z)$ is self-similar under such shifting and rescaling.

of universal functions which is the fixed point of the operator T^*:

$$g_p(z) = [T^* g]_p(z)$$
$$= \alpha g^n_{1+p/\delta}(z/\alpha) \qquad (12.2.24)$$

This universal equation determines both $g_p(z)$ and the universal numbers α and δ. The family of universal functions $g_p(z)$ is called the unstable manifold (the reason is explained in the introductory lectures of Cvitanović[1]).

To summarize, the T^* operation encodes simultaneously the self-similarity of the parameter space (Mandelbrot cactuses) and of the iteration space (Julia sets). Being no more than a redefinition of variables, it is exact, and it is an explicit implementation of the above self-similarities; T^* magnifies the nth iterate of the $(m/n)^{k+1}$-cycle and overlies it onto the $(m/n)^k$-cycle (see Figure 12.4). Asymptotically the self-similarities are exact, and the procedure converges to the unstable manifold, a one-dimensional line of universal functions g_p.

Not only are the N, S, R operations the natural encoding of the complex universality, but they are also useful computational tools.

The universal equation (12.2.24) can be solved numerically by approximating the unstable manifold by a truncation of the double power-series expansion

$$g_p(z) = \sum_{j,k \geq 0} c_{jk} z^{2j} p^k \qquad (12.2.25)$$

We start with equation (12.2.3) as a two-term approximation to $g_p(z)$. Repeated application of the T^* operation (12.2.23) generate a longer and longer double polynomial in z and p; this procedure converges asymptotically to the unstable manifold $g_p(z)$. We implement the shifting and iteration operations S and N as numerical polynomial substitution routines, truncating all polynomials as in expansion (12.2.25). The T operation is completed by the rescaling operation R, in equation (12.2.19). The scaling numbers d and a are fixed by the normalization conditions (12.2.20). We use Newton's method to find the parameter value corresponding to the superstable m/n-cycle. This determines d, and a then follows directly from condition (12.2.20). The result is a new approximation to $g_p(z)$. Asymptotically, the values of d converge to δ and of a converge to α. We keep applying the truncated T^* operation until the coefficients in equation (12.2.25) stabilize to the desired accuracy.

The self-similar structure of the Mandelbrot cactus, Figure 12.1, suggests a systematic way of presenting the universal numbers that we have computed in the previous section. We observe that roughly halfway between any two large leafs on the periphery of a Mandelbrot cactus (such as $\frac{1}{2}$ and $\frac{1}{3}$) there is the next largest leaf (such as $\frac{2}{5}$). Furthermore, we know from equation (12.2.26) that the size of the "cactus leaf" corresponding to period n-tupling is of order n^{-2}. Hence the natural hierarchy is provided by an interpolation scheme, which

organizes rational numbers m/n into self-similar levels of increasing period lengths n. Such a scheme is provided by Farey numbers.[16]

Implicit in the Farey numbers are scaling laws that relate the universal numbers. It turns out that the same Farey structure is a very useful tool for the study of mode-locking intervals for circle maps. We refer the reader to the circle-map references listed in the introduction.

References

1. P. Cvitanović (ed.), *Universality in Chaos*, Hilger, Bristol (1984).
2. B.-L. Hao, *Chaos*, World Scientific, Singapore (1984).
3. M. J. Feigenbaum and R. D. Kenway, in: *Statistical and Particle Physics* (K. C. Bowler and A. J. McKane, eds.), Scottish Universities Summer School in Physics, Dept. of Physics, University of Edinburgh (1984).
4. P. Collet and J.-P. Eckmann, *Iterated Maps on Interval as Dynamical Systems*, Birkhauser, Boston (1980).
5. P. Cvitanović and J. Myrheim, *Commun. Math. Phys.* (to appear).
6. M. H. Jensen, P. Bak, and T. Bohr, *Phys. Rev.* A **30**, 1960 (1984).
7. T. Bohr, M. H. Jensen, and P. Bak, *Phys. Rev. A* **30**, 1970 (1984).
8. S. J. Shenker, *Physica* **5D**, 405 (1982).
9. M. J. Feigenbaum, L. P. Kadanoff, and S. J. Shenker, *Physica* **5D**, 370 (1982).
10. S. Ostlund, D. Rand, J. Sethna, and E. D. Siggia, *Physica* **D8**, 303 (1983).
11. P. Cvitanović, B. Shraiman, and B. Soderberg, *Phys. Scr.* **32**, 263 (1985).
12. A. I. Golberg, Ya. G. Sinai, and K. M. Khanin, *Usp. Mat. Nauk* **38**, 159 (1983).
13. P. Cvitanović and J. Myrheim, *Phys. Lett.* **94A**, 329 (1983).
14. B. B. Mandelbrot, *Ann. N.Y. Acad. Sci.* **357**, 249 (1980).
15. B. B. Mandelbrot, *The Fractal Geometry of Nature*, Freeman, San Francisco (1982).
16. G. H. Hardy and E. M. Wright, *UX (Theory of Numbers)*, Oxford Univ. Press, Oxford (1938).